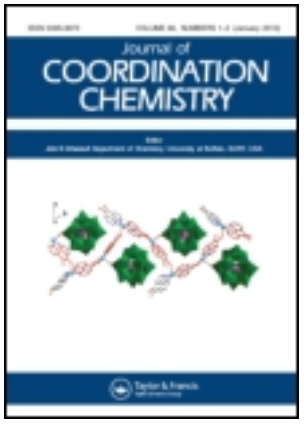

Journal of Coordination Chemistry
Publication details, including instructions for authors and subscription information:
http://www.tandfonline.com/loi/gcoo20

Synthesis, characterization, and mechanism of trans-dichlorido-bis-(ethylenediamine)cobalt(III) with L-cystine in the presence of chloride

Trilochan Swain [a] & Prakash Mohanty [b]

[a] Indic Institute of Design and Research , Bhubaneswar 751004 , Orissa , India

[b] Department of Chemistry , Utkal University , Bhubaneswar 751004 , Orissa , India

Published online: 07 Sep 2011.

To cite this article: Trilochan Swain & Prakash Mohanty (2011) Synthesis, characterization, and mechanism of trans-dichlorido-bis-(ethylenediamine)cobalt(III) with L-cystine in the presence of chloride, Journal of Coordination Chemistry, 64:17, 3051-3061, DOI: 10.1080/00958972.2011.611506

To link to this article: http://dx.doi.org/10.1080/00958972.2011.611506

Journal of Coordination Chemistry
Vol. 64, No. 17, 10 September 2011, 3051–3061

Synthesis, characterization, and mechanism of *trans*-dichlorido-bis-(ethylenediamine)cobalt(III) with L-cystine in the presence of chloride

TRILOCHAN SWAIN*† and PRAKASH MOHANTY‡

†Indic Institute of Design and Research, Bhubaneswar 751004, Orissa, India
‡Department of Chemistry, Utkal University, Bhubaneswar 751004, Orissa, India

(*Received 2 June 2011; in final form 20 July 2011*)

Substitution reactions of *trans*-$[CoCl_2(en)_2]Cl$ (where en = ethylenediamine) with L-cystine has been studied in 1.0×10^{-1} mol dm^{-3} aqueous perchlorate at various temperatures (303–323 K) and pH (4.45–3.30) using UV-Vis spectrophotometer on various $[Cl^-]$ from 0.05 to 0.01 mol L^{-1}. The products have been characterized by their physico-chemical and spectroscopic data. *Trans*-$[CoCl(en)_2(H_2O)]^{2+}$, from the hydrolysis of *trans*-$[CoCl_2(en)_2]^+$ in the presence of Cl^-, formed a complex with L-cystine at all temperatures in 1 : 1 molar ratio. L-cystine is bidentate to Co(III) through Co–N and Co–S bonds. Product formation and reversible reaction rate constants have been evaluated. The rate constants for SN_i mechanism have been evaluated and activation parameters E_a, $\Delta H^{\#}$, and $\Delta S^{\#}$ are determined.

Keywords: L-cystine; SN_i mechanism; Kinetics; Product formation; ^{1}H NMR; XRD

1. Introduction

Transition metal ions and complexes control environmental, industrial, and biological processes [1], increasing the importance of clarifying their mechanistic behavior in simple and complex chemical processes. The structures and reactions of transition metal complexes of cysteine [2], related amino acid thiols, and other amino acids have been studied extensively [3–6]. Reactions between *trans*-$[CoX_2(en)_2]^+$ and amino acid esters [7, 8], or amides [9] gave products in which ester and amide are monodentate, amino-bonded to the metal. Hydrolysis reactions of this complex have also been investigated and, in the case of glycine ester [10, 11] and glycinamide [9] complexes, additional reactions have been reported. By comparison, complexes of the corresponding disulfides have received considerably less attention, because many of them are insoluble and possibly polymeric. Some transition metal complexes containing cystine have been studied for certain biological properties [12]. The substitution of I^- and aqua by cystine [13] are reported for ethylenediamine and diethylenetriamine coordinated square planar Pt(II) complexes. Oxidation of L-cystine by Fe(III), Mn(III), and 12-tungstocobaltate(III) [14] were studied at acidic pH. The cystine is resistant to

*Corresponding author. Email: scienceorissa@rediffmail.com

ISSN 0095-8972 print/ISSN 1029-0389 online
DOI: 10.1080/00958972.2011.611506

oxidation but yields cysteic acid when oxidation occurs with peroxyacetyl nitrate [15]. The importance of sulfur-containing species in biological activity of transition metal complexes prompted us to undertake the present investigation. This reaction of octahedral Co(III) complex in this work has not been reported previously to the best of authors' knowledge. The main objective of this work is to determine the kinetic parameters, SN_i mechanism (nucleophilic substitution intermediate), and characterize substitution products of *trans*-$[CoCl(en)_2(H_2O)]Cl_2$ with cystine at various $[Cl^-]$. The products obtained in 1 : 10 molar ratio have been characterized at pH 3.75 by IR (room temperature), ^1H NMR (308 and 323 K), XRD, and ICP-AES measurements. The product may be used for pharmaceutical activity due to the presence of sulfur-containing amino acid of cystine which is used in biological processes [12].

2. Experimental

Trans-$[CoCl_2(en)_2]Cl$ was synthesized according to the literature [16]. Chemical analysis, UV-Vis, TG-DTA, and ^1H NMR spectroscopic data of this compound are in good agreement with those obtained previously. This compound did not interfere kinetically with perchlorate ion in aqueous solution. So, perchlorate medium was used for kinetics of complex formation reactions. In these reactions, ionic strength of solution was adjusted to 0.1 mol L^{-1} with $NaClO_4$, prepared by neutralizing $HClO_4$ with freshly prepared standardized stock solutions of NaOH in a water bath maintained at ~343 K. $NaClO_4$ was obtained while cooling, as crystals. The $NaClO_4$ stock solution (1 mol dm^{-3}) was adjusted to 6.0 pH and estimated for Na^+ by a combined ion exchange alkalimetric procedure. Analar grade chemicals (E-Merck) were used for all kinetic studies. L-cystine was prepared without purification shortly before use. This ligand was soluble in minimum amount of $HClO_4$ and desired concentration was prepared by adding doubly distilled water. Both complex and ligand were stable under experimental conditions. As *trans*-$[CoCl_2(en)_2]Cl$ was not readily soluble in water, it was kept with doubly distilled water for 2 days with different concentrations of NaCl. As a result some of this complex was transformed to *trans*-$[CoCl(en)_2(H_2O)]^{2+}$ by hydrolysis. Highly purified, deionized water was used in all solutions. The second distillation was made from alkaline $KMnO_4$ using an all glass distillation apparatus.

2.1. *Physical measurements*

The pH measurements were performed using a Nucleonix type DP 301 digital pH meter equipped with a combination of glass-Ag/AgCl, Cl^- (3 mol dm^{-3} NaCl) electrode. This pH meter was calibrated with standard buffers of pH 4.0, 7.0, and 9.0 (Merck). The pH data (i.e., meter readings) at pH <7 were converted to $-\log[H^+]$ by a calibration curve as described earlier [17]. UV-Vis spectra were recorded with a Cecil U.K. model CE-7200 UV/visible spectrophotometer using a cell block housing a pair of 10 mm Quartz Suprasil cells. IR spectra were recorded at room temperature at pH 3.75 with a Shimadzu 8300 FTIR spectrometer. TGA and DTA studies were made using a Shimadzu model DTG 50 (Simultaneous DTA–TG) Thermal Analyzer between 303 and 721 K using an aluminum crucible. ^1H NMR spectra were recorded at 308 and

323 K with pH 3.75 by a 500 MHz spectrometer model UNITY–400, Varian, Switzerland, with D_2O as a solvent in Indian Institute of Chemical Technology (IICT), Hyderabad. XRD and ICP-AES measurements were carried out in SAIF, Kochi. ICP-AES was performed using a Thermo Electron IRIS Intrepid II XSP DUO system for Co and S determination as follows. The sample was dissolved in 5 mL HNO_3 and made up into 100 mL using HPLC grade water. XRD measurement (powder form) was carried out with a Bruker AXS D8 Advance at room temperature.

2.2. *Kinetic measurements*

All activation parameters were determined by Arrhenius and Eyring equations from temperature variation experiments. Reactions were studied on a Cecil U.K. model CE-7200 UV/visible spectrophotometer. Constant temperature was maintained by an external circulating thermostat (±273.01 K) connected to a Peltier. The reactions were monitored under pseudo-first order conditions as follows. The reaction of cystine and *trans*-$[CoCl(en)_2(H_2O)]^{2+}$ were studied using ligand in excess (≥10-fold). All reactions were studied in perchlorate medium with total ionic strength of 1.0×10^{-1} mol dm^{-3} with different temperatures (303, 308, 313, 318, and 323 K) and $[H^+]$. The ionic strength as well as pH adjusted solution of the reaction mixture was thermally equilibrated in a 10 cm^3 measuring flask and then a known volume (1 cm^3) of the stock complex solution was added. This reaction mixture was quickly (*ca.* ≤10 s) transferred to the cell placed in the thermostated cellblock of the spectrophotometer. The reactions were followed for at least 75% of reaction at wavelengths where respective absorbance changes were the largest. Spectral changes resulting from mixing of complex and ligand solution were recorded between 320 and 650 nm. At pH 4.00, the repetitive spectral scans of the reaction mixture of *trans*-$[CoCl(en)_2(H_2O)]^{2+}$ and L-cystine displayed a steady decrease of absorbance with time at 370 nm (figure S1) (instead of 300 nm for hydrolysis of *trans*-$[CoCl_2(en)_2]^+$ without chloride ion). Progress of reaction was monitored at a pre-selected wavelength by recording absorbance with time against water; cystine was varied from 1.0 to 3.0×10^{-3} mol dm^{-3} and NaCl was varied from 0.01 to 0.05 mol L^{-1} while *trans*-$[CoCl(en)_2(H_2O)]^{2+} = 1.0 \times 10^{-4}$ mol dm^{-3} was kept constant. Linear kinetic traces were collected in all cases from absorbance (A_t)–time (t,s) data and observed pseudo-first order rate constants k_{obs} were evaluated from slope by fitting of equation $Y = m\ X + C$ by plotting $\ln(A_t - A_\infty)$ *versus* time (s) (where A_t and A_∞ were absorbance of different time intervals and at final). The rate constants, k_p (product constant), were evaluated by plotting $\ln(A_t - A_{t,t})$ *versus* time [13]. This plot was nonlinear. The reversible rate constants, k_r (s^{-1}), were evaluated by plotting $\ln\{(A_o - A_t)/(A_o - A_{50})\}$ *versus* time and observed value was deducted from the product rate constant (k_p). The plot $\ln\{(A_o - A_t)/(A_o - A_{50})\}$ *versus* time was nonlinear (A_{50} is absorbance at 50 min), curved at the initial stage, and subsequently of constant slope indicating that both product formation and reversible reaction proceed through two parallel steps. The double exponential rise to max method of five parameters was adopted to calculate the rate constant for two parallel steps. The k_{obs} values were evaluated by fitting the absorbance–time data sets to the two exponential equation:

$$Y = Y_0 + A(1 - e^{-bx}) + C(1 - e^{-dx}). \quad (1)$$

The terms A and C were composed of rate constants and absorbance. For SN_i mechanism, the rate constants were evaluated by plotting $[\{\ln(A_t - A_{t,t})\} - A_\infty]$ *versus* time ($A_{t,t}$ is absorbance at time where absorbance starts to decrease). This plot was linear and rate constant was evaluated. Data fitting involved 50 data points in most cases. All calculations were made on a PC using linear and nonlinear least-squares programs.

3. Results and discussion

3.1. *Reaction products*

The products are obtained by mixing *trans*-$[CoCl(en)_2(OH_2)]^{2+}$ with cystine in 1 : 10 molar ratio at pH 3.75. The reaction mixtures are heated at 308 and 323 K for about 24 h and dried in silica gel desiccators. The crystals obtained are recrystallized from doubly distilled water at room temperature after filtering. The pinkish white square crystals obtained are highly hygroscopic. Finally, it is dried in silica gel desiccators.

3.1.1. UV-Vis spectra. From UV-Vis spectra, 330–726 nm, the product has three bands in the visible spectrum, λ_{max} 374 nm ($A_{1g} \rightarrow T_{2g},O_h$), 522 nm ($A_{1g} \rightarrow T_{1g},O_h$), and 596 nm, indicating that the product is *trans*-configuration [18]. The d–d transition at 596 nm indicated sulfur coordination to Co(III) center [19].

3.1.2. IR spectra results. The spectra of *trans*-$[CoCl(en)_2(OH_2)]^{2+}$ with cystine at pH 3.75 are presented in figure S2. At pH 3.75, the S–S symmetric stretch remained intact at 480 cm^{-1} with very low intensity [20], indicating that peptide bond did not break during reaction. Peaks at 630, 939, and 1087 cm^{-1} were assigned for Co(III)–N stretch, CH_2 rocking, and C–C stretch of ethylene diamine [21]. Absorption at 1145 cm^{-1} was assigned for C–C stretch of cystine, which remained intact [20]. The COO^- stretch of cystine and C=O antisymmetric stretch remained intact at 1489 cm^{-1} and 1585 cm^{-1}, respectively, but the intensity decreased remarkably [22], perhaps due to intramolecular hydrogen-bonding with NH_3^+. The NH_2 stretch shifted from 2096 cm^{-1} [21] to 2017 cm^{-1} revealing Co(III)–NH_2 bond formation. The NH_2 asymmetric stretch shifted from 3429 to 3414 cm^{-1}.

3.1.3. ^{1}H NMR spectra results. This product was soluble in D_2O and readily characterized by ^{1}H NMR spectroscopy (figures S3 and S4). The ^{1}H NMR data of the product are collected in table 1. Spectra were collected at 308 K and 323 K at pH 3.75. The ^{1}H NMR peaks (at 308 K) appeared δ (ppm): 1.40 {2H, triplet, CH_2 (ethylenediamine)}, 1.00 {2H, doublet, CH_2 (cystine)} and 1.20 {2H, doublet, CH_2 (cystine)}, 2.80–3.20 {1H, multiplet, CH (cystine)} and 5.40 (singlet, intramolecular hydrogen-bonding between NH_3^+ and COO^-). At 323 K the peaks shifted downfield, δ (ppm): 1.60 {2H, triplet, CH_2 (ethylenediamine)}, 1.10–1.20 {2H, doublet, CH_2 (cystine)} and 1.40 {2H, doublet, CH_2 (cystine)}, 2.90–3.40 {1H, multiplet, CH (cystine)}. From pH 3.30 to 4.45, two donors of cystine, one sulfur of (S–S) and one amine (NH_2), bonded Co(III) at both temperatures. The proposed product structures at

Table 1. ^{1}H NMR of product at pH 3.75 at 308 and 323 K in D_2O.

	δen (ethylenediamine)	δ cystine	
Temp. (K)	CH^2	CH^2	CH
308	1.40 (triplet)	1.00 (doublet) 1.20 (doublet)	2.80–3.20 (multiplet)
323	1.60 (triplet)	1.10–1.20 (doublet) 1.40 (doublet)	2.90–3.40 (multiplet)

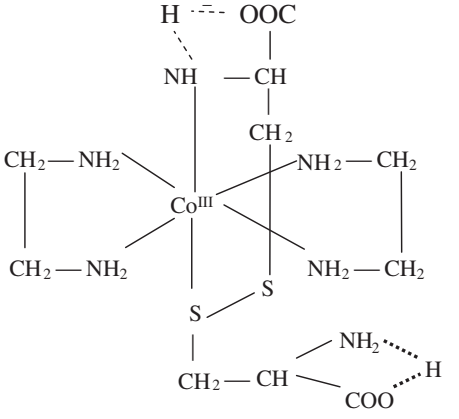

Figure 1. The proposed product of *trans*-$[Co(en)_2(N,S,cystine)]^{2+}$ at low temperature.

308 and 323 K are shown in figure 1. From TG-DTA spectrum (figure S5), the product formed 1 : 1 complex with cystine at pH 4.45. From TG-DTA spectrum of *trans*-$[CoCl_2(en)_2]ClO_4$, the melting point was sharp at ~521 K (figure S6).

3.1.4. X-ray diffraction. To determine the crystal structure of cobalt complex, X-ray diffraction data are collected at room temperature with graphite-monochromated MoK_α radiation on an XPERT PRO diffractometer operating in $\omega/2\theta$ scan mode. The cell parameters are determined from a least-squares refinement of 15 centered reflections. Crystal data and experimental details of the title complex are collected in table 2. The XRD spectrum is shown in figure S7.

The C–N bond length of cystine was 1.15276 Å, similar to Felice *et al.* [23], and this plane was obtained at an angle of 41.93°. The C–O bond distance of cystine was 1.26393 Å instead of 1.239 Å [23] and this plane was obtained at an angle of 37.54°. The C–C bond length of ethylene diamine was 1.41151 Å and made an angle of 33.07°. This was found similar to Schubert *et al.* [24]. The Co^{III}–N(cystine) bond length was similar to cobalt(III) imido bond lengths of 1.62931 Å [25] and this plane made an angle of 28.21°. The C–S bond length of cystine was 1.70268 Å instead of 1.73 Å [26] and this plane made an angle of 26.89°. The Co^{III}–N(ethylene diamine) bond length was 1.99710 Å, which was found similar to Becker *et al.* [27] and this plane made an angle

Table 2. Crystal data and experimental details of the title compound.

Empirical formula	$Co_1N_6C_{10}S_2O_4H_{27}$
Molecular mass (g)	417.9
Temperature (K)	298
Wavelength (Å)	1.542475
Crystal color	Pinkish white
θrange for data collection (°)	3.0000–90.0050
Number of points	9500
Scan axis	Gonio
Scan step size	0.01
Time per step	0.5
Scan type	Continuous
$K\alpha_2/K\alpha_1$	0.5
h k l	0 0 0

of 22.68°. In cystine, intermolecular interactions of $NH_3^+ \ldots O$ with bond length 2.82579 Å against 2.812 Å were observed [28]. This plane made an angle of 15.81°. The oxidized state of the C_H3 domain has $S_\gamma - S_\gamma$ within a conventional covalent disulfide bond distance of 2.0 Å [29]. This distance increased to 3.25731 Å, similar to the model reduced state [30].

3.1.5. ICP-AES analysis. The elemental analysis of complex was carried out by ICP-AES. The Co and S were consistent with the theoretical values. Anal. Calcd for $\{Co^{III}(en)_2(cystine)\}$ is S: 15.31%; Co^{III}: 14.10%; found S: 15.30%; Co^{III}: 14.13%.

4. Kinetic analysis

In order to determine the contribution from possible reaction paths between *trans*-$[CoCl(en)_2(OH_2)]^{2+}$ and *trans*-$[CoCl_2(en)_2]^+$, complex formation with cystine is studied at different $[H^+]$, temperatures, [cystine], and $[Cl^-]$.

4.1. *Effect of hydrogen ion concentration*

Under conditions $[Co(III)] = 1.0 \times 10^{-4}$, $[\text{L-cystine}] = 1.0 - 3.0 \times 10^{-3}$, $I = 1.0 \times 10^{-3}\,\text{mol dm}^{-3}$ ($NaClO_4$), pH is varied from 3.30 to 4.45 at 303–323 K, and $[Cl^-]$ from 0.05 to 0.01 mol L^{-1}. The pseudo first-order rate constant, k_{obs} ($6.641 \times 10^{-4}\,s^{-1}$) is optimum at pH 4.45, $T = 323$ K and $[\text{cystine}] = 3.0 \times 10^{-3}\,\text{mol dm}^{-3}$ with 0.05 mol L^{-1} NaCl; $k_{obs}(s^{-1})$ increased with increase in pH from 3.30 to 4.45. The pseudo first-order rate constants, $k_{obs}(s^{-1})$, are evaluated from absorbance *versus* time graphs as follows:

$$k_{obs} = \frac{[Cl^-][\text{cystine}]K_a^2 k_1}{[H^+]\{K_a + [\text{cystine}]\}} + \{k_{-1} + [\text{cystine}]\} \times \sigma, \quad (2)$$

where K_a (cystine) $= 10^{-2.05}$ and $\sigma =$ steric effect. The steric effect is observed at low temperature on cystine depending on $[H^+]$ and $[Cl^-]$. This effect is eliminated at higher

Table 3. Rate constants k_1 and k_{-1} for the substitution between Co(III) with cystine from pH 3.30 to 4.45 at 1.0×10^{-1} mol dm^{-3} $NaClO_4$ on 0.05–0.01 mol L^{-1} NaCl medium.

		0.05 mol L^{-1}		0.03 mol L^{-1}		0.01 mol L^{-1}	
Temp. (T/K)	pH	$k_1 \times 10^2$ ((mol L^{-1})$^{-1}$ s^{-1})	$k_{-1} \times 10^5$ (s^{-1})	$k_1 \times 10^2$ ((mol L^{-1})$^{-1}$ s^{-1})	$k_{-1} \times 10^5$ (s^{-1})	$k_1 \times 10^2$ ((mol L^{-1})$^{-1}$ s^{-1})	$k_{-1} \times 10^5$ (s^{-1})
303	4.45	2.52 ± 0.06	0.45 ± 0.01	1.46 ± 0.12	2.63 ± 0.01	0.80 ± 0.10	1.68 ± 0.01
308		5.59 ± 0.06	1.00 ± 0.01	3.24 ± 0.12	5.82 ± 0.02	1.63 ± 0.11	3.45 ± 0.01
313		8.66 ± 0.06	1.56 ± 0.02	5.36 ± 0.12	9.67 ± 0.03	2.47 ± 0.10	5.21 ± 0.01
318		12.55 ± 0.06	2.26 ± 0.04	8.69 ± 0.12	15.60 ± 0.04	4.44 ± 0.10	9.37 ± 0.01
323		13.81 ± 0.06	2.48 ± 0.06	12.69 ± 0.12	22.81 ± 0.07	7.99 ± 0.10	16.86 ± 0.02
303	4.40	1.79 ± 0.05	0.32 ± 0.01	1.51 ± 0.11	2.72 ± 0.01	0.74 ± 0.10	1.07 ± 0.01
308		3.17 ± 0.05	0.57 ± 0.01	2.62 ± 0.11	4.71 ± 0.01	1.41 ± 0.10	2.13 ± 0.02
313		6.38 ± 0.05	1.15 ± 0.01	4.24 ± 0.10	7.64 ± 0.02	2.27 ± 0.10	3.31 ± 0.02
318		9.58 ± 0.05	1.72 ± 0.01	7.54 ± 0.10	13.53 ± 0.02	4.02 ± 0.11	5.90 ± 0.01
323		10.54 ± 0.05	1.89 ± 0.01	11.17 ± 0.11	20.05 ± 0.04	7.13 ± 0.10	10.55 ± 0.01
303	3.75	1.59 ± 0.02	0.28 ± 0.01	1.54 ± 0.10	2.77 ± 0.01	0.69 ± 0.10	0.46 ± 0.01
308		2.81 ± 0.02	0.50 ± 0.01	2.30 ± 0.11	4.15 ± 0.01	1.19 ± 0.11	0.81 ± 0.01
313		4.99 ± 0.03	0.90 ± 0.01	3.68 ± 0.11	6.63 ± 0.01	2.07 ± 0.10	1.41 ± 0.01
318		7.17 ± 0.03	1.29 ± 0.03	6.97 ± 0.10	12.49 ± 0.01	3.61 ± 0.10	2.44 ± 0.01
323		10.30 ± 0.03	1.85 ± 0.05	10.42 ± 0.10	18.67 ± 0.02	6.27 ± 0.11	4.24 ± 0.01
303	3.30	1.96 ± 0.24	0.35 ± 0.01	1.57 ± 0.10	2.82 ± 0.01	0.67 ± 0.11	0.46 ± 0.01
308		2.50 ± 0.24	0.45 ± 0.01	1.99 ± 0.11	3.60 ± 0.01	1.03 ± 0.10	0.69 ± 0.01
313		3.18 ± 0.24	0.57 ± 0.03	3.13 ± 0.11	5.62 ± 0.01	1.76 ± 0.10	1.19 ± 0.01
318		5.65 ± 0.24	10.17 ± 0.06	6.39 ± 0.10	11.46 ± 0.02	3.31 ± 0.10	2.24 ± 0.01
323		10.70 ± 0.24	19.23 ± 0.11	9.66 ± 0.10	17.30 ± 0.02	5.8 ± 0.11	3.93 ± 0.01

temperature due to lack of intramolecular hydrogen-bonding. σ values were 1.92 and 1.70 for 0.01 and 0.03 mol L^{-1} [Cl$^-$], respectively, at [cystine] = 2 and 3×10^{-3} mol dm^{-3} at high temperature. At [Cl$^-$] = 0.05 mol L^{-1}, the σ values were 1.50 and 3.05 at low and high temperatures, respectively.

Mono-aqua complex concentration was lower than that of dichloride complex due to high chloride concentration. On rearranging equation (2),

$$k_{obs} = \left(\left\{ \frac{[Cl^-][\text{cystine}]K_a^2 k_1}{[H^+]\{K_a + [\text{cystine}]\}} + K_a \right\} [\text{cystine}] + k_{-1} \right) \times \sigma \tag{3}$$

with the steric effect caused by [H$^+$] and [Cl$^-$] on cystine is given below.

$$\text{Steric factor} = \frac{[Cl^-]K_a^2}{[H^+]\{K_a + [\text{cystine}]\}} + K_a. \tag{4}$$

The second-order rate constants, k_1 (mol L^{-1})$^{-1}$ s^{-1}), are evaluated in NaCl medium by plotting k_{obs} *versus* [L-cystine]. Based on these experiments and taking total concentration of nucleophiles, the following mechanism can be formulated:

$$-\text{d [structures (I) and (II) of scheme 1][Nu]/d}t = k_1 [\text{cystine}] + k_{-1}. \tag{5}$$

The plot of k_{obs} *versus* [cystine] was linear with intercept k_{-1}. The rate constants, k_1 ((mol L^{-1})$^{-1}$ s^{-1}), are evaluated from the slope. The rate constants k_1 and k_{-1} are summarized in table 3. As [H$^+$] increases, the first-order reversible rate constants, k_{-1}, decrease indicating that both mono-aqua and dichloride complexes have lower

reversible rate constant at low pH. The second-order rate constants, k_1, increase with increase in pH and turned optimum, $k_1 = 1.38 \times 10^{-1}\,(\mathrm{mol\,L^{-1}})^{-1}\,\mathrm{s^{-1}}$, at pH 4.45 on $T = 323\,\mathrm{K}$ and $[\mathrm{Cl^-}] = 0.05\,\mathrm{mol\,L^{-1}}$.

4.1.1. Product formation. Product formation was nonlinear in plots of absorbance *versus* time. The k_{obs} values are evaluated by fitting absorbance–time data sets in a two-exponential equation:

$$Y = Y_0 + E(1 - e^{-k\mathrm{obs3}x}) + F(1 - e^{-k\mathrm{obs4}x}), \tag{6}$$

E and F are composed of rate constants and absorbance. The pseudo first-order rate constant, k_{obs3} ($1.86 \times 10^{-2}\,\mathrm{s^{-1}}$), is optimum at pH 4.45 and $T = 323\,\mathrm{K}$ having [cystine] $= 3.0 \times 10^{-3}\,\mathrm{mol\,dm^{-3}}$ and $[\mathrm{Cl^-}] = 0.01\,\mathrm{mol\,L^{-1}}$.With increasing $[\mathrm{H^+}]$, k_{obs3} decreased due to decrease of active secondary amine groups of cystine ($\mathrm{pK_2} = 2.04$). The k_{obs4} ($2.03 \times 10^{-3}\,\mathrm{s^{-1}}$) is optimum at pH 4.45 and $T = 323\,\mathrm{K}$ having [cystine] $= 3.0 \times 10^{-3}\,\mathrm{mol\,dm^{-3}}$ and $[\mathrm{Cl^-}] = 0.05\,\mathrm{mol\,L^{-1}}$. With increasing $[\mathrm{H^+}]$, k_{obs4} decreased at all $[\mathrm{Cl^-}]$. The rate constants k_{obs3} and k_{obs4} are evaluated from equation (6).

4.1.2. Reversible reaction. The reversible reaction was also nonlinear in plotting $\ln\{(A_o - A_t)/(A_o - A_{50})\}$ *versus* time. The k_{obs} values are evaluated by fitting the absorbance–time data sets in the two-exponential equation:

$$Y = Y_0 + G(1 - e^{-k\mathrm{obs}-3x}) + H(1 - e^{-k\mathrm{obs}-4x}), \tag{7}$$

the two terms G and H are composed of rate constants and absorbance. The pseudo-first order reversible rate constant, $k_{\mathrm{obs}-4}$ ($5.52 \times 10^{-5}\,\mathrm{s^{-1}}$), is optimum at pH 4.45 with $[\mathrm{Cl^-}] = 0.01\,\mathrm{mol\,L^{-1}}$ having [cystine] $= 3.0 \times 10^{-3}\,\mathrm{mol\,dm^{-3}}$ and $T = 323\,\mathrm{K}$. With increasing $[\mathrm{H^+}]$, $k_{\mathrm{obs}-4}$ decreases at all $[\mathrm{Cl^-}]$; $k_{\mathrm{obs}-3}$ ($7.86 \times 10^{-4}\,\mathrm{s^{-1}}$) is optimum at pH 4.45 with $[\mathrm{Cl^-}] = 0.01\,\mathrm{mol\,L^{-1}}$ having [cystine] $= 3.0 \times 10^{-3}\,\mathrm{mol\,dm^{-3}}$ on $T = 323\,\mathrm{K}$. With increasing $[\mathrm{H^+}]$, these pseudo-first order reversible rate constants decreased. The pseudo-first order reversible rate constants $k_{\mathrm{obs}-3}$ and $k_{\mathrm{obs}-4}$ are evaluated from equation (7).

4.2. *Effect of [Cl⁻]*

$[\mathrm{Cl^-}]$ varied from 0.01 to $0.05\,\mathrm{mol\,L^{-1}}$ and k_{-1} and k_1 increase with increasing $[\mathrm{Cl^-}]$, as per scheme 1. $k_{\mathrm{obs3}} > k_{\mathrm{obs4}}$ at all pH for each $[\mathrm{Cl^-}]$. Pseudo-first order rate constants, k_{obs4}, increase at all pH and concentrations of dichloride increases due to prevention of spontaneous solvolytic processes by excess $[\mathrm{Cl^-}]$. The rate constants, k_{obs3}, decrease with increasing $[\mathrm{Cl^-}]$ due to decrease in concentration of mono-aqua complex as $[\mathrm{Cl^-}]$ increases, preventing formation of solvolytic process.

For the reversible reaction, pseudo-first order reversible rate constants, $k_{\mathrm{obs}-3}$, decreased with increasing $[\mathrm{Cl^-}]$. Similarly, $k_{\mathrm{obs}-4}$ decreased with increasing $[\mathrm{Cl^-}]$. In these reversible reactions, $\mathrm{k_{obs-3}} > \mathrm{k_{obs-4}}$ at all pH of each $[\mathrm{Cl^-}]$. The reaction was more favorable at high $[\mathrm{Cl^-}]$.

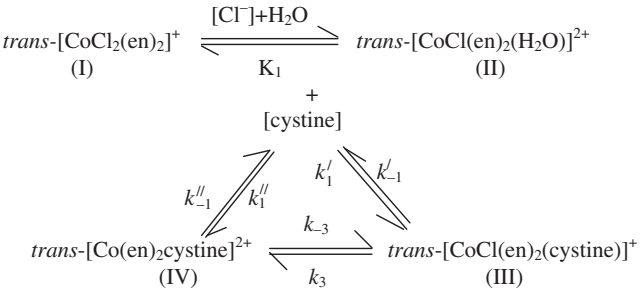

Scheme 1. In the presence of Cl^- both (I) and (II) depend upon $[Cl^-]$. Structure (I) reacts with cystine to form (IV) while in the presence of $[Cl^-]$ (II) reacts with cystine to form (III) which further reacted to form (IV). Here $k_1 = k_1' + k_1''$; $k_{-1} = k_{-1}' + k_{-1}''$; $k_4 = k_1''$ and $k_{-4} = k_{-1}''$.

Table 4. Activation parameters of forward reactions at pH from 3.30–4.45 having $[Cl^-] = 0.01$–$0.05\,mol\,L^{-1}$.

pH	$[Cl^-]$ ($mol\,L^{-1}$)	$\Delta H^{\#}$ ($kJ\,mol^{-1}$)	$\Delta S^{\#}$ ($JK^{-1}\,mol^{-1}$)	E_a ($kJ\,mol^{-1}$)
3.30	0.05	65 ± 2	-110 ± 6	68
3.75		73 ± 2	-80 ± 6	76
4.00		73 ± 1	-81 ± 3	76
4.45		74 ± 1	-79 ± 3	68
3.30	0.03	75 ± 2	-80 ± 6	77
3.75		77 ± 1	-72 ± 3	80
4.00		79 ± 1	-64 ± 4	82
4.45		83 ± 1	-49 ± 3	86
3.30	0.01	86 ± 1	-53 ± 3	88
3.75		87 ± 1	-49 ± 3	89
4.00		88 ± 1	-43 ± 3	90
4.45		88 ± 2	-39 ± 6	91

4.3. *Effect of temperature*

Activation parameters ($\Delta H^{\#}$ and $\Delta S^{\#}$) are computed using a weighted program of the Eyring equation; E_a is computed using the Arrhenius equation. The negative entropy at all pH of each $[Cl^-]$ suggests that the activation process is dominated by bond making, indicating substitution followed an I_a mode of activation [31]. The activation parameters and k_{obs}SNi suggest that for L-cystine a pentagonal bipyramidal transition state formed at Co^{III}. All activation parameter values are tabulated in table 4.

5. SN_i mechanism

Normally, I_a and I_d mechanisms cannot be distinguished from traditional kinetic analysis. From our SN_i mechanism calculation, it was possible to distinguish between

$$\underset{\text{(I)}}{\textit{trans}\text{-}[CoCl_2(en)_2]^+ + (S,N,cys)} \xrightarrow{k_{obs}SNi} \underset{\text{(II)}}{cys,S,N,\text{----}Co(en)_2\text{-----}2Cl^-} \longrightarrow \underset{\text{(III)}}{product}$$

Scheme 2. The SN_i mechanism for $[CoCl_2(en)_2]Cl$ with cystine in the presence of Cl^-. The k_{obs}SNi was linear at all pH and $[Cl^-]$. In step (I) cystine approached Co(III) and formed partial bond-like structure (II) and in the last step $2Cl^-$ leave Co(III) and formed product.

these mechanisms. The k_{obs}SNi are evaluated from the slope by plotting $[\{\ln(A_t - A_{t,t})\} - A_\infty]$ *versus* time of:

$$\text{time } (t, s) = \text{slope} \times [\{\ln(A_t - A_{t,t})\} - A_\infty] + C, \tag{8}$$

and k_{obs}SNi ($7.14 \times 10^{-4}\,s^{-1}$) was optimum at pH 4.45 of $[Cl^-] = 0.05\,mol\,L^{-1}$, $T = 323\,K$, and [cystine] $= 3.0 \times 10^{-3}\,mol\,dm^{-3}$. The k_{obs}SNi decreased on increasing $[H^+]$ and increased with increase in $[Cl^-]$ (i.e., increase in $[Cl^-]$ facilitates removal of existing ligands and approach of cystine to Co(III) increased). The steric factor increased with increase in $[H^+]$ due to hydrogen-bonding, decreasing the approach of cystine to [Co(III)]. k_{obs}SNi $> k_{obs}$ at all pH and $[Cl^-]$, indicating that association with ligand took place before substitution, as per scheme 2. The negative entropy also revealed associative I_a mechanism.

6. Product mechanism

The rate of product formation is observed as below at particular pH as

$$\begin{aligned} d/dt\{\textit{trans}\text{-}[Co(en)_2(cystine)]^{2+}\} = \{&k_3 \times \textit{trans}\text{-}[CoCl(en)_2(cystine)]^+ - k_{-3} \times \textit{trans}\text{-}\\ &[Co(en)_2(cystine)]^{2+}\} + k_1^{//}[cystine][\textit{trans}\text{-}CoCl(en)_2H_2O]^{2+}\\ &- k_{-1}^{//}[\textit{trans}\text{-}Co(en)_2(cystine)]^{2+}\}. \end{aligned} \tag{9}$$

Putting $\textit{trans}\text{-}[CoCl(en)_2(cystine)]^+$ in equation (9),

$$\begin{aligned} -d/dt\ \textit{trans}\text{-}[CoCl_2(en)_2]^+ = \{&k_1^{//} \times \textit{trans}\text{-}[CoCl_2(en)_2]^+[cystine]^+ - k_{-1}^{//} \times \textit{trans}\text{-}\\ &[Co(en)_2(cystine)]^{2+}\} + k_1^{/}K_1 \times \textit{trans}\text{-}[CoCl_2(en)_2]^+[cystine] - k_1^{/}K_1 \times \textit{trans}\text{-}\\ &[CoCl_2(en)_2]^+[cystine]. \end{aligned}$$

On rearranging the above equation, the rate of disappearance is:

$$= \textit{trans}\text{-}[CoCl_2(en)_2]^+[cystine]\ \{k_1^{//} + 2k_{-1}^{/}K_1\} - k_{-1}^{//}\ \textit{trans}\text{-}[Co(en)_2(cystine)]^{2+}.$$

Acknowledgments

The author is grateful to Department of Chemistry, Utkal University for providing necessary lab. facility. The author thanks Department of Pharmaceutical Science for providing IR spectrum.

References

[1] (a) L. Dyers, S.Y. Que, D. VanDerveer, X.R. Bu. *Inorg. Chim. Acta*, **359**, 197 (2006); (b) M.A.U. Daula, J.A. Khanam, A.Y.K.M. Masud Rana. *J. Med. Sci.*, **4**, 124 (2004); (c) P. Kamalakannan, D. Venkappayya. *J. Inorg. Biochem.*, **21**, 22 (2002).
[2] B.V. Petrovic, Z.D. Bugarcic. *Aust. J. Chem.*, **58**, 544 (2005).
[3] S.K. Bera, G.S. De. *Indian J. Chem., Sect. A*, **43**, 1882 (2004).
[4] (a) S.K. Bhattacharya, R.N. Banerjee. *Polyhedron*, **16**, 4217 (1997); (b) P.C. Jocelyn. *Biochemistry of the SH Group*, pp. 77–85, Academic Press, London (1972).
[5] (a) A. Khan, Kabir-ud-Din. *Int. J. Chem. Kinet.*, **17**, 1263 (1985); (b) M. Friedman. *The Chemistry and Biochemistry of the Sulfhydryl Group in Amino Acids, Peptides and Proteins*, Chap. 2, Pergamon Press, New York (1973).
[6] (a) I.A. Khan, Kabir-ud-Din, M. Sahid. *J. Indian Chem. Soc.*, **69**, 864 (1992); (b) J.P. Greenstein, M. Winitz. *Chemistry of the Amino Acids*, pp. 638–645, Wiley, New York (1961).
[7] M.D. Alexander, D.H. Busch. *Inorg. Chem.*, **5**, 602 (1966).
[8] R.W. Hay, R. Bennett, D.J. Barnes. *Dalton Trans.*, 1524 (1972).
[9] D.A. Buckingham, D.M. Foster, A.M. Sargeson. *J. Am. Chem. Soc.*, **92**, 6151 (1970).
[10] D.A. Buckingham, D.M. Foster, A.M. Sargeson. *J. Am. Chem. Soc.*, **91**, 4102 (1969).
[11] M.D. Alexander, D.H. Busch. *J. Am. Chem. Soc.*, **88**, 1130 (1966).
[12] J.A. Khanam, F.B. Most, J. Ara, M. Jesmin, M.A. Taher, S.M.M. Ali. *J. Pharm. Sci.*, **5**, 29 (2006).
[13] (a) D.K. Baral, G.S. Brahma, T. Swain, M. Sahu, P. Mohanty. *J. Indian Chem. Soc.*, **83**, 131 (2006); (b) T. Swain, P. Mohanty. *Aust. J. Chem.*, **62**, 493 (2009).
[14] (a) R.F. Jameson, W. Linert, A. Tschinkowitz, V. Gutmann. *Dalton Trans.*, 943 (1988); (b) N. Annapurna, A.K. Kumar, P. Vani, G.N. Rao. *Transition Met. Chem.*, **33**, 691 (2008); (c) P.K. Satpathy, G.C. Dash, P. Mohanty. *Indian J. Chem. Soc., Sect. A*, **47A**, 1199 (2008).
[15] F. Leh, J.B. Mudd. *Arch. Biochem. Biophys.*, **161**, 216 (1974).
[16] M. Krishnamurthy. *J. Inorg. Nucl. Chem.*, **34**, 3915 (1972).
[17] (a) H.M. Irving, M.G. Miles, L.D. Pettit. *Anal. Chim. Acta*, **38**, 475 (1967); (b) A. Das, A.C. Dash. *Dalton Trans.*, **12**, 1949 (2000).
[18] M.D. Alexander, D.H. Husch. *Inorg. Chem.*, **5**, 1590 (1966).
[19] V.M. Kothari, D.H. Busch. *Inorg. Chem.*, **8**, 2276 (1969).
[20] M. Jesmin, M.M. Ali, A.K. Biswas, M.R. Habib, J.A. Khanam. *Med. J. Islamic World Acad. Sci.*, **16**, 135 (2007).
[21] K. Nakamoto. *Infrared and Raman Spectra of Inorganic and Coordination Compounds*, 5th Edn, p. 18, Wiley, New York (1997).
[22] E. Ramachandran, S. Natarajan. *Cryst. Res. Technol.*, **39**, 308 (2004).
[23] R.D. Felice, A. Sellori, E. Molinari. *J. Phys. Chem. B*, **107**, 1151 (2003).
[24] U. Schubert, B. Zimmmer-Gasser, K.C. Dash, G.T. Chaudhury. *Cryst. Struct. Commun.*, **10**, 239 (1981).
[25] R.E. Cowley, R.P. Bontchev, J. Sorrell, O. Sarracino, Y. Feng, H. Wang, J.M. Smith. *J. Am. Chem. Soc.*, **129**, 2424 (2007).
[26] Ok-S. Jung, Y.T. Kim, Y-J. Kim, J.K. Chon, H.K. Chae. *Bull. Korean Chem. Soc.*, **20**, 648 (1999).
[27] K.A. Becker, G. Grosse, K. Plieth. *Z. Kristallogr.*, **112**, 375 (1959).
[28] B. Koleva, M. Spiteller, T. Kolev. *Amino Acids*, **38**, 295 (2010).
[29] E.O. Saphire, P.W. Parren, R. Pantophlet, M.B. Zwick, G.M. Morris, P.M. Rudd, R.A. Dwek, R.L. Stanfield, D.R. Burton, I.A. Wilson. *Science*, **293**, 1155 (2001).
[30] A. Mcauley, J. Jacob, C.G. Kolven Bach, K. Westland, H.J. Lee, S.R. Brych, D. Rehder, G.R. Kleemann, D.N. Brems, M. Matsumura. *Protein Sci.*, **17**, 95 (2008).
[31] M.L. Tobe, J. Burgess. *Inorganic Reaction Mechanisms*, Vol. 70, Addison Wesley Longman, Harlow, England (1999).